



Trade Science Inc.

# Nano Science and Nano Technology

An Indian Journal

Full Paper

NSNTAIJ, 7(5), 2013 [197-203]

## New nano-sized supramolecular metal coordination polymers derived from 1,2-bis (2-pyridyl)-ethene and benzimidazole

Aref A.M.Aly\*, Maged S.Al-Fakeh, Mahmoud A.Ghandour, B.M.Abu-Zied  
Chemistry Department, Faculty of Science, Assiut University, 71516 Assiut, (EGYPT)  
E-mail : maged7969@yahoo.com

### ABSTRACT

A number of new nano-sized supramolecular coordination polymers of Mn (II), Co (II), Ni (II), Cu (II) and Cd (II) derived from 1,2-bis (2-pyridyl) ethene (BPE) and benzimidazole (BIMZ) has been prepared and characterized. The compounds have been characterized based on elemental analysis, FT-IR and electronic spectral studies and thermal analysis. Thermogravimetry (TG), derivative thermogravimetry (DTG) and differential thermal analysis (DTA) have been used to study the thermal decomposition steps and to calculate the thermodynamic parameters of the metal coordination polymers. The kinetic parameters have been calculated from the Coats-Redfern and Horowitz-Metzger equations. From SEM and TEM photographs as well as from the powder XRD data the particle size of the complexes was determined which indicates the nano-sized nature of the prepared compounds (average size 24-28 nm).

© 2013 Trade Science Inc. - INDIA

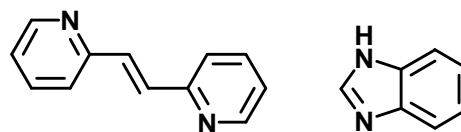
### KEYWORDS

Coordination polymers;  
X-ray powder diffraction;  
Thermal studies SEM and  
TEM.

### INTRODUCTION

Supramolecular Coordination polymers have received much attention due to their potential applications as functional materials ranging from gas storage<sup>[1,2]</sup>, ion-exchange<sup>[3-5]</sup>, magnetism<sup>[6]</sup>, catalysis<sup>[7]</sup> and molecular sensing<sup>[8,9]</sup>. The continuing interest in this area is also due to their intriguing variety of architectures and topologies through the variation of building blocks and reaction conditions<sup>[10-14]</sup>. Bidentate bridging ligands such as 1,2-bis (4-pyridyl)ethane and 1,2-bis (2-pyridyl)ethene are widely used to construct stable supramolecular complexes of well designed self-assembly<sup>[15]</sup>. These complexes are of potential application in catalysis<sup>[16]</sup>. In the last decade coordination com-

pounds with infinite one-, two-, and three-dimensional network structures have been intensively studied<sup>[17-19]</sup>. In last decades, heterocyclic benzimidazoles, their derivatives and transition metal complexes have received considerable attention in coordination chemistry, because of their well-documented biological activities. It was found that such complexes showed larger antimicrobial activities than the free ligands<sup>[20,21]</sup>. The aim of this article is therefore to synthesize and



1,2-bis(2-pyridyl)ethene benzimidazole

Figure 1 : Structures of the ligands.

## Full Paper

characterize a number of new nano-sized of metal supramolecular coordination polymers derived from 1,2-bis (2-pyridyl)ethene and benzimidazole to explore their structures and properties. The structures of the ligands are presented in Figure 1.

## EXPERIMENTAL

### Material

High purity 1,2-bis (2-pyridyl)ethene (BPE) and benzimidazole (BIMZ) were purchased from Sigma Aldrich and Merck grade. All other chemicals were of AR grade.

### Physical measurements

The stoichiometric analyses (C,H,N) were performed using Analytischer Funktionstest Vario El Fab-Nr.11982027 elemental analyzer. The conductance was measured using a conductivity Meter model 4310 JENWAY. The i.r spectra were recorded on a Shimadzu IR-470 spectrophotometer and the electronic spectra were obtained using a Shimadzu UV-2101 PC spectrophotometer. Thermal studies were carried out in dynamic air on a Shimadzu DTG 60-H thermal analyzer at a heating rate 10 °C min<sup>-1</sup>. The x-ray diffractometer was a Philips 1700 version with H. T. P.W 1730 / 104 KVA. The anode was Cu K $\alpha$  ( $\lambda = 1.54180 \text{ \AA}$ ). The scanning electron microscope was a JEOL JFC-1100E ION SPUTTERING DEVICE, JEOL JSM-5400LV SEM. SEM specimens were coated with gold to increase the conductivity. Transmission electron microscope (JEOL JEM-100CX II ELECTRON MICROSCOPE).

### Syntheses of the complexes

Synthesis of the mixed ligand supramolecular coordination polymers of BPE and BIMZ with Mn (II),

Co (II), Ni (II), Cu (II) and Cd (II) follows essentially the same procedure. [Co (BPE)(BIMZ)Cl<sub>2</sub>(H<sub>2</sub>O)]<sub>n</sub> synthesis is typical. An ethanolic solution (15 ml) of BPE (0.2 g, 1.1 mmol) was slowly added into a hot ethanolic solution (15 ml) of cobalt (II)chloride 1.1 mmol and then a ethanolic solution (15 ml) of BIMZ (0.13 g, 1.1 mmol) was added dropwise. The resultant mixture was stirred for 1 h and filtered and then cooled to room temperature. The blue precipitate was separated, washed with distilled water and EtOH and then dried over CaCl<sub>2</sub> in a desiccator.

## RESULTS AND DISCUSSION

The supramolecular coordination polymers were prepared by the reaction of BPE, metal chlorides and BIMZ in stoichiometric proportions to yield the corresponding compounds according to the following equation:



These components were found to react in the molar ratio 1: 1: 1 metal : BPE : BIMZ. The complexes are air stable, insoluble in common organic solvents but partially soluble in DMSO or DMF. The molar conductivity values  $\Lambda_m$  of the complexes in 10<sup>-3</sup> M DMSO solutions vary from 11.49 to 48.36 S cm<sup>2</sup> mol<sup>-1</sup>, thus revealing their non-electrolytic character<sup>[22]</sup>. The compositions of the complexes are supported by the elemental analysis recorded in TABLE 1.

### IR spectra

The most relevant infrared spectral bands of the ternary complexes are given in TABLE 2. The bands

TABLE 1 : Colors, elemental analysis and melting points of the compounds.

Compound	M.F (M.Wt)	Color	Found (Calcd.%)			m.p. °C (Decom.)	$\Lambda_m$ Scm <sup>2</sup> mol <sup>-1</sup>
			C	H	N		
{[Mn (BPE)(BIMZ)Cl <sub>2</sub> (H <sub>2</sub> O)].3H <sub>2</sub> O} <sub>n</sub> 1	C <sub>19</sub> H <sub>23</sub> Cl <sub>2</sub> MnN <sub>4</sub> O <sub>4</sub> (497.3)	Light-brown	46.32 45.88	5.43 4.67	10.63 11.26	238	24.56
[Co (BPE)(BIMZ)Cl <sub>2</sub> (H <sub>2</sub> O)] <sub>n</sub> 2	C <sub>19</sub> H <sub>17</sub> Cl <sub>2</sub> CoN <sub>4</sub> O (447.23)	Blue	52.10 51.02	3.90 3.83	11.21 12.53	209	48.36
[Ni (BPE)(BIMZ)Cl <sub>2</sub> (H <sub>2</sub> O)] <sub>n</sub> 3	C <sub>19</sub> H <sub>17</sub> Cl <sub>2</sub> NiN <sub>4</sub> O (446.99)	Light- green	50.87 51.05	3.77 3.84	11.90 12.53	218	20.82
{[Cu (BPE)(BIMZ)Cl <sub>2</sub> (H <sub>2</sub> O)].4H <sub>2</sub> O} <sub>n</sub> 4	C <sub>19</sub> H <sub>25</sub> Cl <sub>2</sub> CuN <sub>4</sub> O <sub>5</sub> (523.93)	Light- blue	44.91 43.55	4.74 4.81	9.63 10.69	224	12.89
{[Cd (BPE)(BIMZ)Cl <sub>2</sub> (H <sub>2</sub> O)].2H <sub>2</sub> O} <sub>n</sub> 5	C <sub>19</sub> H <sub>21</sub> CdN <sub>4</sub> Cl <sub>2</sub> O <sub>3</sub> (536.75)	White	43.20 42.51	4.92 3.95	9.66 10.44	230	11.49

observed in the 1611–1618  $\text{cm}^{-1}$  regions are assigned to the  $\delta$  (C=N) stretching vibration of the 1,2-bis(2-pyridyl)ethene<sup>[16,23]</sup>. Furthermore, BIMZ exhibits the bands in the region 1426–1437  $\text{cm}^{-1}$  which can be assigned to  $\delta$  (C-N) ring<sup>[24]</sup>. A band with medium intensity located in the range 3180–3200  $\text{cm}^{-1}$  may be assigned to  $\nu$  (OH) for the coordinated  $\text{H}_2\text{O}$  in all compounds<sup>[25]</sup>. For complexes 1, 4 and 5 the  $\nu$ OH stretching vibration of lattice  $\text{H}_2\text{O}$  appears at the 3420–3490  $\text{cm}^{-1}$ <sup>[26]</sup>. Metal-oxygen and metal-nitrogen bonding are manifested by the appearance of a band in the 518–528  $\text{cm}^{-1}$  and 419–438  $\text{cm}^{-1}$  regions, respectively<sup>[26]</sup>.

TABLE 2 : Infrared spectral data of the complexes.

Compound	Y (OH) lattice	Y (OH) coord.	Y (N-H)	Y (C-N)	Y (C=N)	Y (M-N)	Y (M-O)
1	3490	3190	3136	1436	1613	428	519
2	-	3196	3110	1437	1612	432	518
3	-	3200	3090	1430	1618	436	518
4	3420	3190	3130	1432	1616	438	528
5	3450	3180	3123	1426	1611	419	520

### Electronic spectra and magnetic moments

The UV-Vis spectra of the complexes have been recorded in DMSO. The results are shown in TABLE 3. For all the complexes a band appearing in the range 23,809–35,716  $\text{cm}^{-1}$  which can be attributed to the  $n \rightarrow \delta^*$  transition. The band occurring in the range 33,670–40,322  $\text{cm}^{-1}$  is assigned, however, to a  $\delta \rightarrow \delta^*$  transition. The metal complexes except Cd (II) show broad bands with very low intensity in the range 25,000–12,000  $\text{cm}^{-1}$ , which are assigned to the d-d transitions. That no transitions were observed in the visible region for complex 5 is consistent with the  $d^{10}$  configuration of  $\text{Cd}^{2+}$ . For Mn (II), the magnetic moment value of 5.60 B.M is in agreement with the value reported for those of Mn (II) octahedral complexes<sup>[27]</sup>. The magnetic moment value of 4.36 B.M for the Co (II) complex indicates an octacoordination around Co (II)<sup>[28]</sup>. However, the magnetic moment value of 2.70 B.M. confirms the paramagnetic nature of the Ni (II) complex and the octahedral geometry around Ni (II) ion<sup>[29]</sup>. The observed magnetic moment value of 1.91 B.M. for the Cu (II) complex signifies the octahedral

environment around Cu (II) ion<sup>[30]</sup>. (TABLE 3). From the above data the structure of the complexes can be postulated as follows:

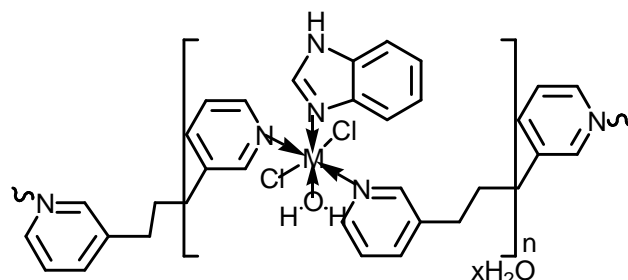


Figure 2 : Structure of  $\{[M(\text{BPE})(\text{BIMZ})\text{Cl}_2(\text{H}_2\text{O})]_n \cdot x\text{H}_2\text{O}\}_n$  M = Mn (II), Co (2+), Ni (II), Cu (II) and Cd (II), x = 2, 3 or 4.

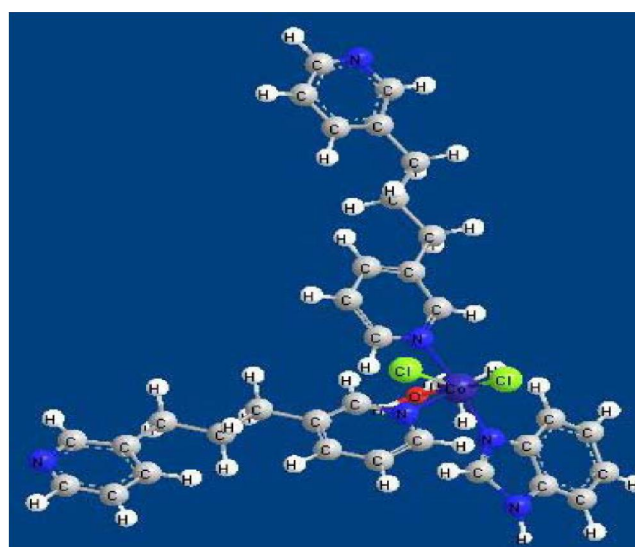


Figure 3 : View of the complete coordination around the metal ions in the coordination polymers.

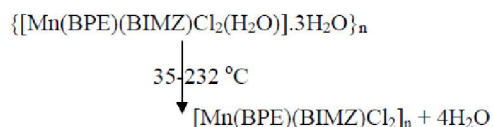
TABLE 3 : Electronic spectral data and magnetic moments of the compounds.

Compounds	$\nu_{\text{max}}$ ( $\text{cm}^{-1}$ )	Assignment	$\mu_{\text{eff}}$ B.M
1	18,115	d-d transition	5.60
	23,809	$n \rightarrow \pi^*$ transition	
	40,322	$\pi \rightarrow \pi^*$ transition	
2	21,367	d-d transition	4.36
	29,761	$n \rightarrow \pi^*$ transition	
	37,037	$\pi \rightarrow \pi^*$ transition	
3	18,248	d-d transition	2.70
	24,752	$n \rightarrow \pi^*$ transition	
	36,496	$\pi \rightarrow \pi^*$ transition	
4	15,230	d-d transition	1.91
	27,777	$n \rightarrow \pi^*$ transition	
	33,670	$\pi \rightarrow \pi^*$ transition	
5	35,716	$n \rightarrow \pi^*$ transition	-
	36,630	$\pi \rightarrow \pi^*$ transition	

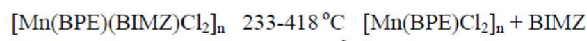
## Full Paper

### Thermal properties of the complexes

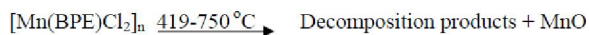
The complexes were subjected to a TG analysis in dynamic air from 50 to 750 °C. The thermal decomposition data of the compounds are collected in TABLE 4. The complexes are relatively thermally stable. They decompose in multistage processes. As a representative example the thermogram of the manganese complex 1 in dynamic air is shown in Figure 4. They show that the thermal decomposition processes of the complex involve five stages. The first and second stages is a dehydration process occurring in the temperature range from 35 to 232 °C. The mass loss (calc. 14.49 %, found 13.53 %) indicates the loss of 4H<sub>2</sub>O molecules water (coordinated and three crystalline) and formation of the anhydrous complex [Mn(BPE)(BIMZ)Cl<sub>2</sub>]. For this steps (DTG minimum at 108, 213 °C) an endothermic broad peaks is observed in the DTA at 109, 214 °C in the curve.



The observed mass losses of the third step (233-418 °C) in the TG curve agree with the decomposition of the benzimidazole (calc. 23.75 %, found 23.06 %). This step is marked on the DTG curve a peaks at (382 °C) corresponding to the broad exothermic peak in the DTA curve at 383 °C.



The forth and fifth stages (419-502 °C) and (503-750 °C) in the TG curve corresponding to decomposition product with corresponding two DTG peaks at 494 and 521 °C and two exothermic peaks at 495 and 522 °C in the DTA trace, respectively. The ultimate product at 750 °C is consistent with the formation of MnO (calc. 14.26 %, found 14.21 %).



### Kinetic analysis

Non-isothermal kinetic analysis of the complexes was carried out applying two different procedures: the Coats-Redfern<sup>[31]</sup> and the Horowitz-Metzger<sup>[32]</sup> methods.

#### Coats-redfern equation

$$\ln[1-(1-\alpha)^{1-n}/(1-n)T^2] = M/T + B \quad \text{for } n \neq 1 \quad (2)$$

$$\ln[-\ln(1-\alpha)/T^2] = M/T + B \quad \text{for } n = 1 \quad (3)$$

where  $\alpha$  is the fraction of material decomposed,  $n$  is the order of the decomposition reaction and  $M = -E/R$  and  $B = ZR/\dot{O}E$ ;  $E$ ,  $R$ ,  $Z$  and  $\dot{O}$  are the activation energy, gas constant, pre-exponential factor and heating rate, respectively.

TABLE 4: Thermal decomposition data of the compounds in dynamic air.

Compounds	Step	TG/DTG			Mass Loss (%)
		Ti	Tm	Tf	
1	1 <sup>st</sup>	35	108	130	5.15
	2 <sup>nd</sup>	131	213	232	8.38
	3 <sup>rd</sup>	233	382	418	23.06
	4 <sup>th</sup>	419	494	502	32.91
	5 <sup>th</sup>	503	521	750	16.29
2	1 <sup>st</sup>	30	99	141	4.01
	2 <sup>nd</sup>	142	205	294	26.02
	3 <sup>rd</sup>	295	537	550	26.62
	4 <sup>th</sup>	551	578	750	27.81
4	1 <sup>st</sup>	32	60	152	3.23
	2 <sup>nd</sup>	153	200	263	12.75
	3 <sup>rd</sup>	264	364	385	50.36
	4 <sup>th</sup>	386	603	750	19.18

Ti=Initial temperature, Tm=Maximum temperature, Tf=Final temperature.

### Horowitz-metzger equation

$$\ln[1-(1-\alpha)^{1-n}/1-n] = \ln ZRT_s^2/\Phi E - E/RT_s + E\theta/RT_s^2 \quad \text{for } n \neq 1 \quad (4)$$

$$\ln[-\ln(1-\alpha)] = E\theta/RT_s^2 \quad \text{for } n = 1 \quad (5)$$

where  $\theta = T-T_s$ ,  $T_s$  is the temperature at the DTG peak. The correlation coefficient  $r$  is computed using the least squares method for equations (2), (3), (4) and (5). Linear curves were drawn for different values of  $n$  ranging from 0 to 2. The value of  $n$ , which gave the best fit, was chosen as the order parameter for the decomposition stage of interest. The kinetic parameters were calculated from the plots of the left hand side of equations (2), (3), against  $1/T$  and against  $\theta$  for equations (4) and (5). The kinetic parameters for the compounds 1, 2 and 4 are calculated for the first step according to the above two methods and are cited in TABLE 5. The Thermodynamic parameters entropy ( $\Delta S^*$ ), enthalpy ( $\Delta H^*$ ) and free energy ( $\Delta G^*$ ) of activation were calculated using the following standard relations:

$$\Delta S^* = R [\ln Zh / kTs] \quad (6)$$

$$\Delta H^* = \Delta E^* - RT_s \quad (7)$$

$$\Delta G^* = \Delta H^* - T_s \Delta S^* \quad (8)$$

where:  $h$ , Planck's constant,  $k$ , Boltzmann constant,  $R$ , gas constant,  $T_s$ , Temperature at the DTG peak. Negative  $\Delta S^*$  value for the different stages of decomposition of the complexes suggest that the activated complex is more ordered than the reactants and that the reactions are slower than normal<sup>[33-35]</sup>. The more ordered nature may be due to the polarization of bonds in the activated state, which might happen through charge transfer electronic transition<sup>[36]</sup>. The different values of  $\Delta H^*$  and  $\Delta G^*$  of the complexes refer to the effect of the struc-

ture of the metal ions on the thermal stability of the complexes<sup>[37]</sup>. The positive values of  $\Delta G^*$  indicate that the decomposition reaction is not spontaneous (TABLE 6).

### X-ray powder diffraction of the complexes

The X-ray powder diffraction patterns were recorded for the following coordination polymers 1 and 5. The diffraction patterns indicate that the compounds are crystalline. The crystal lattice parameters were computed with the aid of the computer program TREOR.

TABLE 5 : Kinetic parameters for the thermal decomposition of the coordination polymers (1, 2 and 4) in dynamic air.

Compound	Step	Coats-Redfern equation				Horowitz-Metzger equation			
		$r$	$n$	$E$	$Z$	$r$	$n$	$E$	$Z$
1	1st	1	0.33	56.1	$11.29 \times 10^2$	1	0.33	71.5	$4.43 \times 10^3$
2	1st	0.9984	2.00	108.7	$29.80 \times 10^2$	0.9997	2.00	118.5	$28.83 \times 10^4$
4	1st	1	0.66	31.7	$6.40 \times 10^2$	1	0.66	41.5	$5.22 \times 10^4$

$E$  in  $\text{kJ mol}^{-1}$

TABLE 6 : Thermodynamic parameters for the thermal decomposition of the compounds (1, 2 and 4) in dynamic air.

Compound	Step	$\Delta G^*$	$\Delta H^*$	$\Delta S^*$
1	1 <sup>st</sup>	-196.59	30.68	128.0
2	1 <sup>st</sup>	-192.73	35.41	127.92
4	1 <sup>st</sup>	-202.23	11.28	140.50

$\Delta H^*$ ,  $\Delta G^*$  are in  $\text{kJ mol}^{-1}$  and  $\Delta S^*$  in  $\text{kJ mol}^{-1} \text{K}^{-1}$

The crystal data for all metal mixed-ligand complexes belong to the crystal system triclinic. The significant broadening of the peaks indicates that the particles are of nanometer dimensions (RD of compounds 1 and 5 is depicted in Figures 5 and 6). Scherrer's equation (6) was applied to estimate the particle size of the coordination polymers:

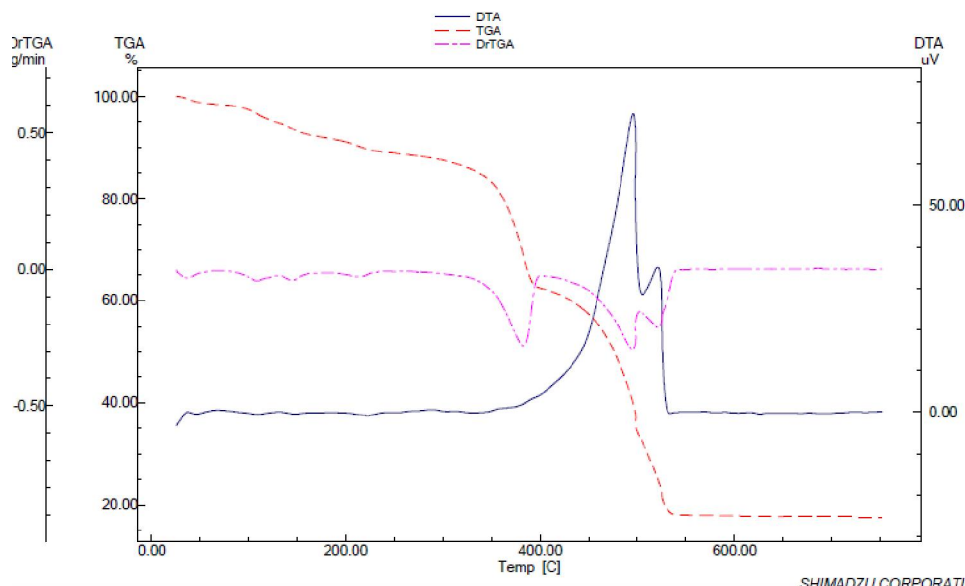


Figure 4 : TG, DTG and DTA thermograms of  $\{[Mn (BPE)(BIMZ)Cl_2(H_2O)].3H_2O\}_n$  in dynamic air.

$$D = K\lambda / \beta \cos\theta \quad (9)$$

where  $K$  is the shape factor,  $\lambda$  is the X-ray wavelength typically  $1.54 \text{ \AA}$ ,  $\beta$  is the line broadening at half the maximum intensity in radians and  $\theta$  is Bragg angle,  $D$  is

the mean size of the ordered (crystalline) domains, which may be smaller or equal to the grain size. The Scherrer's equation is limited to nano scale particles. The crystal data together with particle size are recorded in TABLE

## Full Paper

**TABLE 7 : X-ray diffraction crystal data of the compounds 1, 5 and their particle size.**

Parameters	1	5
Empirical formula	C <sub>19</sub> H <sub>23</sub> MnN <sub>4</sub> O <sub>4</sub> Cl <sub>2</sub>	C <sub>19</sub> H <sub>21</sub> CdN <sub>4</sub> O <sub>3</sub> Cl <sub>2</sub>
Formula weight	497.30	536.75
Crystal system	triclinic	triclinic
a (Å)	6.198	4.678
b (Å)	9.156	9.416
c (Å)	9.073	14.746
α (°)	80.763	52.742
β (°)	82.613	88.774
γ (°)	103.157	72.732
Volume of unit cell (Å <sup>3</sup> )	487.66	482.96
Particle size (nm)	28	24

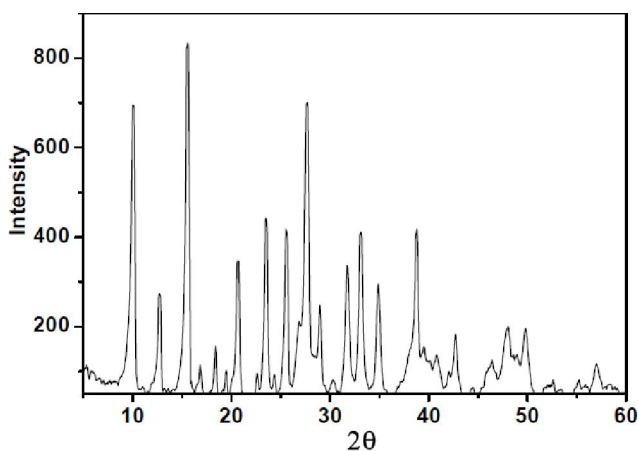


**Figure 5 : XRD of {[Mn (BPE)(BIMZ)Cl<sub>2</sub>(H<sub>2</sub>O)].3H<sub>2</sub>O}<sub>n</sub> 1.**

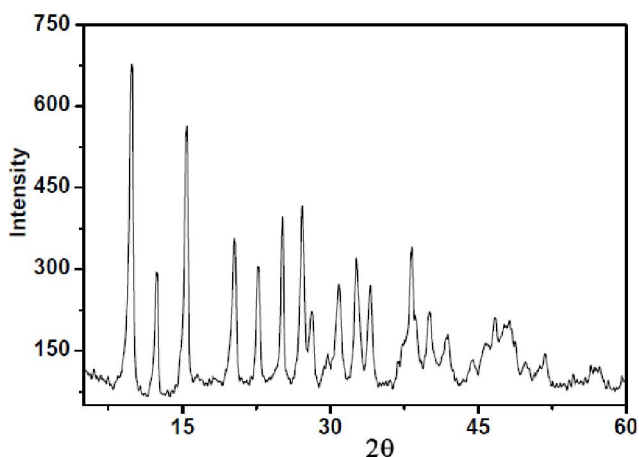


**Figure 6 : XRD of {[Cd (BPE)(BIMZ)Cl<sub>2</sub>(H<sub>2</sub>O)].2H<sub>2</sub>O}<sub>n</sub> 5.**

7. The average size of the particles lies in the range 24–28 nm which is in agreement with that observed by scanning electron microscope.

### Electron microscopies (SEM & TEM)

The scanning electron micrographs of Mn (II) and

Cd (II) mixed ligand complexes as representatives are given in Figures 7 and 8. The figures show the different morphologies of the complexes.

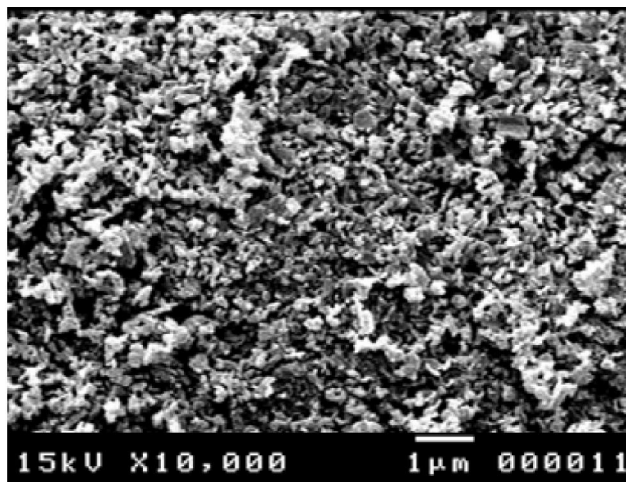


**Figure 7 : SEM of {[Mn (BPE)(BIMZ)Cl<sub>2</sub>(H<sub>2</sub>O)].3H<sub>2</sub>O}<sub>n</sub>**

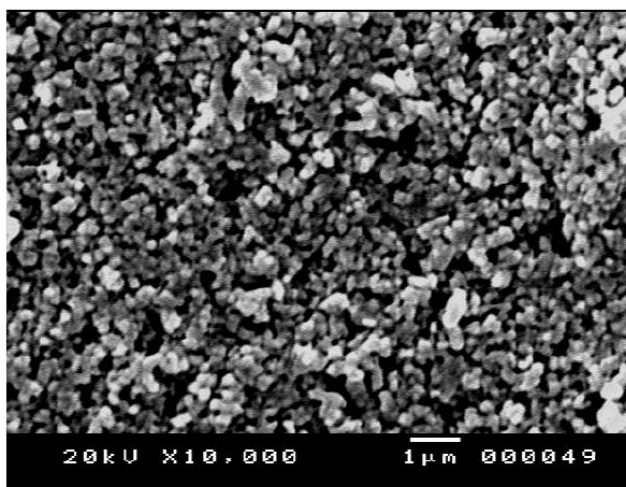


**Figure 8 : SEM of {[Cd (BPE)(BIMZ)Cl<sub>2</sub>(H<sub>2</sub>O)].2H<sub>2</sub>O}<sub>n</sub>**

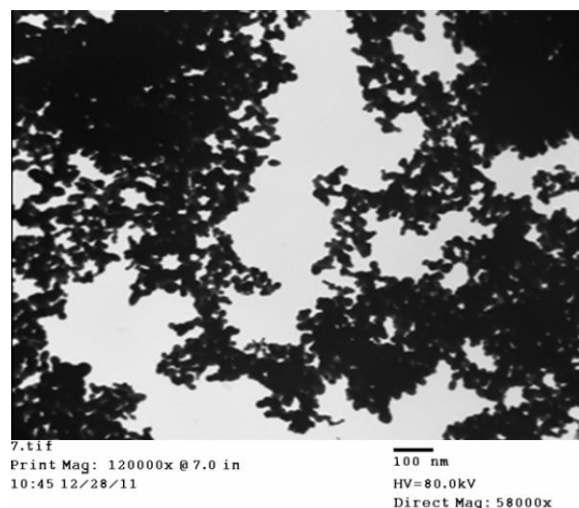


**Figure 9 : TEM of {[Cd (BPE)(BIMZ)Cl<sub>2</sub>(H<sub>2</sub>O)].2H<sub>2</sub>O}<sub>n</sub>**

Figure 9 shows TEM nanographs of as-prepared nanocrystalline by calcined at 500 °C. The particle sizes of Cd (II) compound are in the range 18-27 nm. These results are in a good agreement with the sizes determined from XRD analysis by the Scherrer's equation (TABLE 7).

### ACKNOWLEDGEMENT

One of the authors (A.A.M.ALY) is very grateful to Alexander Von Humboldt Foundation for donating the magnetic susceptibility balance (MSB-Auto).

### REFERENCES

- [1] K.S.Min, M.P.Suh; *J.Am.Chem.Soc.*, **122**, 6834 (2000).
- [2] J.Fan, L.Gan, H.Kawaguchi, W.Y.Sun, K.B.Yu, W.X.Tang; *Chem.Eur.J.*, **9**, 3965 (2003).
- [3] A.J.Fletcher, E.J.Cussen, D.Bradshaw, M.J.Rosseinsky, K.M.J.Thomas; *Am.Chem.Soc.*, **126**, 9750 (2004).
- [4] B.Kesanli, Y.Cui, M.R.Smith, E.W.Bittner, B.C.Bockrath, W.Lin; *Angew.Chem.Int.Ed.*, **44**, 72 (2005).
- [5] H.Chun, D.N.Dybtssev, H.Kim, K.Kim; *Chem.Eur.J.*, **11**, 3521 (2005).
- [6] G.A.Mines, B.C.Tzeng, K.J.Stevenson, J.Li, J.T.Hupp; *Angew.Chem.Int.Ed.*, **41**, 154 (2002).
- [7] S.Hasegawa, S.Horike, R.Matsuda, S.Furukawa, K.Mochizuki, Y.Kinoshita, S.J.Kitagawa; *Am.Chem.Soc.*, **129**, 2607 (2007).
- [8] M.C.Hong, Y.J.Zhao, W.P.Su, R.Cao, M.Fujita, Z.Y.Zhou, A.S.C.Chan; *J.Am.Chem.Soc.*, **122**, 4819 (2000).
- [9] J.F.Ma, J.F.Liu, X.Yan, H.Q.Jia, Y.H.Lin; *J.Chem.Soc.Dalton Trans.*, **1**, 2403 (2000).
- [10] S.R.Batten, R.Robson; *Angew.Chem.Int.Ed.*, **37**, 1460 (1998).
- [11] K.Kim; *Chem.Soc.Rev.*, **31**, 96 (2002).
- [12] C.Janiak; *Dalton Trans.*, 2781 (2003).
- [13] S.Noro, R.Kitaura, M.Komdo, S.Kitagawa, T.Ishii, H.Matsuzaka, M.Yamashita; *J.Am.Chem.Soc.*, **124**, 2568 (2002).
- [14] S.L.James; *Chem.Soc.Rev.*, **32**, 276 (2003).
- [15] Z.Ozhamam, M.Yurdakul, S.Yurdakul; *Vibr.Spect.*, **43**, 335 (2007).
- [16] S.H.Kim, B.K.Park, Y.J.Song, S.M.Y, H.G.Koo, E.Y.Kim, J.I.Poong, J.H.Lee, S.J.Kim, Y.Kim; *Inorg.Chim.Act.*, **362**, 4119 (2009).
- [17] S.Koner, S.Saha, T.Mallah, K.Okamoto; *Inorg.Chem.*, **43**, 840 (2004).
- [18] (a) E.Q.Gao, S.Q.Bai, Y.F.Yue, Z.M.Wang, C.H.Yan; *Inorg.Chem.*, **42**, 3642 (2003); (b) E.Q.Gao, Y.F.Yue, S.Q.Bai, Z.He, C.H.Yan; *Chem.Mater*, **16**, 1590 (2004).
- [19] A.Escuer, M.Font-Bardý'a, S.S.Massoud, F.A.Mautner, E.Peñalba, X.Solans, R.Vicente; *New J.Chem.*, **28**, 681 (2004).
- [20] F.Gumus, O.Algul, G.Eren, H.Eroglu, N.Diril, S.Gur, A.Ozkul; *Eur.J.Med.Chem.*, **38**, 473 (2003).
- [21] D.Kumar Sau, R.J.Butcher, S.Chaudhuri, N.Saha; *Molec.Cell.Biochem.*, **253**, 21 (2003).
- [22] W.J.Geary; *Coord.Chem.Rev.*, **7**, 81 (1971).
- [23] J.Qiang, W.Ping, Y.Yu, W.Huan, W.Hong, Q.Zhang, J.Miller; *Inorg.Chim.Act.*, **362**, 1295 (2009).
- [24] K.S.Banu, S.Mondal, A.Guha, S.Das, T.Chattopadhyay, E.Suresh, E.Zangrando, D.Das; *Polyhedron*, **30**, 163 (2011).
- [25] A.Bravo, J.Anacona; *Transition.Met.Chem.*, **26**, 20 (2001).
- [26] T.Rakha; *Synth.React.Inorg.Met.Org.Chem.*, **30**, 205 (2000).
- [27] M.C.Jain, R.K.Sharma, P.C.Jain; *Gazz.Chim.Ital.*, **109**, 601 (1979).
- [28] A.B.P.Lever; *Inorganic Electronic Spectroscopy*, 2nd Editions, Elsevier, Amsterdam, (1984).
- [29] A.A.El-Asmy, M.Mounir; *Transition Met.Chem.*, **13**, 143 (1988).
- [30] J.R.Anacona, C.Toledo; *Transition Met.Chem.*, **26**, 228 (2001).
- [31] A.Coats, J.Redfern; *Nature*, **20**, 68 (1964).
- [32] H.Horowitz, G.Metzger; *Anal.Chem.*, **35**, 1464 (1963).
- [33] G.G.Mohamed, W.M.Hosny, M.A.Abd El-Rahim; *Syn.and React.in Inorg.and Metal-Org.Chem.*, **32**, 1501 (2000).
- [34] M.A.Beg, M.A.Qaiser; *Thermochimica Acta*, **210**, 123 (1998).
- [35] O.P.Pandey, S.K.Sengupta, S.C.Tripathi; *A review Thermochimica Acta*, **96**, 155 (1985).
- [36] K.M.Yusuff, A.R.Karthikeyan; *Thermochimica Acta*, **207**, 93 (1992).
- [37] M.E.Emam, M.Kanawy, M.H.Hafe; *J.of Therm.Anal.and Calori.*, **63**, 75 (2001).